Author Manuscript

Author Manuscript

Author Manuscript

Author Manuscript

HHS Public Access

Author manuscript

Mov Disord. Author manuscript; available in PMC 2023 April 01.

Published in final edited form as:

Mov Disord. 2022 April ; 37(4): 847–853. doi:10.1002/mds.28895.

Disruption of brainstem structural connectivity in REM sleep behavior disorder using 7 Tesla MRI

María Guadalupe García-Gomar, MD, PhD[1], **Aleksandar Videnovic, MD, MSc**[2,3], **Kavita Singh, PhD**[1], **Matthew Stauder**[2], **Laura D. Lewis, PhD**[1], **Lawrence L. Wald, PhD**[1], **Bruce R. Rosen, MD, PhD**[1], **Marta Bianciardi, PhD**[1,3]

[1]Department of Radiology, Athinoula A. Martinos Center for Biomedical Imaging, Massachusetts General Hospital and Harvard Medical School, Boston, MA, United States

[2]Department of Neurology, Massachusetts General Hospital and Harvard Medical School, Boston, MA, United States

[3]Division of Sleep Medicine, Harvard University, Boston, MA

Abstract

Background: Isolated REM-sleep-behavior-disorder (iRBD) is one of the earliest manifestations of alpha synucleinopathies. Brainstem pathophysiology underlying REM-sleep-behavior-disorder has been described in animal models, yet it is understudied in living humans due to the lack of an in-vivo brainstem nuclei atlas and to the limited MRI sensitivity.

Objective: To investigate brainstem structural connectivity changes in iRBD patients by using an in-vivo probabilistic brainstem nuclei atlas and 7 Tesla MRI.

Methods: Structural connectivity of twelve iRBD patients and twelve controls was evaluated by probabilistic tractography. Two-sided Wilcoxon rank-sum test was used to compare the structural-connectivity-indices across groups.

Results: In iRBD, we found impaired ($Z=2.6$, $p<0.01$) structural connectivity in 14 brainstem nuclei, including the connectivity between REM-on (e.g. subcoeruleus) and REM-sleep muscle-atonia (e.g. medullary reticular formation) areas.

Conclusions: The brainstem nuclei diagram of impaired connectivity in human iRBD expands animal models and is a promising tool to study and possibly assess prodromal synucleinopathy stages.

Corresponding Authors: María Guadalupe García-Gomar, MD, Ph.D. mgarciagomar@mgh.harvard.edu Department of Radiology, Athinoula A. Martinos Center for Biomedical Imaging, Massachusetts General Hospital and Harvard Medical School, Building 149, Room 2132, 13th Street, Charlestown, MA 02129, USA. Phone: +1 617 726 0305, Marta Bianciardi, Ph.D. martab@mgh.harvard.edu Department of Radiology, Athinoula A. Martinos Center for Biomedical Imaging, Massachusetts General Hospital and Harvard Medical School, Building 149, Room 2301, 13th Street, Charlestown, MA 02129, USA. Phone: +1 617 724 1723; Fax: +1 617 726 7422.

Author Roles

MGGG, MB organized and executed the project. MGGG, AV, KS, MS, MB wrote the manuscript. MB secured the funding. AV, LL, LW, BR gave feedback along the process.

Financial Disclosure/Conflict of Interest: The authors declare that the research was conducted in the absence of any commercial or financial relationships that could be construed as a potential conflict of interest.

Author Manuscript Author Manuscript Author Manuscript Author Manuscript

Keywords

Isolated REM-sleep-behavior-disorder; premanifest-synucleinopathy; brainstem; 7 Tesla MRI; tractography

Introduction

Isolated rapid-eye-movement (REM) sleep behavior disorder (iRBD) is a sleep disorder characterized by the absence of muscular atonia and dream enactment behaviors during REM-sleep[1]. iRBD patients have up to 73.5% risk of developing a neurodegenerative synucleinopathy (including Parkinson's disease, multiple system atrophy and dementia with Lewy bodies) after 12 years from iRBD-diagnosis[2]. Thus, iRBD allows the investigation of early, premanifest stages of synuclein-specific neurodegeneration when treatment can be most effective in arresting its progression. Changes in the brainstem nuclei microstructure and connectivity are expected in iRBD, based on studies in animals and in patients with brainstem lesions[3]. These changes are also expected based on *ex-vivo* human staging models of synucleinopathy progression[4] (Fig. 1A), which predict early deposition of alpha-synuclein in caudal brainstem nuclei in premanifest stages. Nevertheless, brainstem changes underlying iRBD are currently understudied in living humans due to difficulty in localizing brainstem nuclei in conventional images and lack of an *in-vivo* atlas of these regions.

The objective of our work was to investigate the presence of structural connectivity changes of brainstem nuclei in iRBD using high angular-resolution diffusion imaging (HARDI) at 7 Tesla, as well as a recently developed probabilistic structural atlas of brainstem nuclei of the arousal and motor systems in Montreal-Neurological-Institute (MNI) space[5,6], expanded in the current work to include all brainstem nuclei relevant for iRBD/premanifest-synucleinopathy.

Methods

Subjects

Twelve patients with iRBD (age 68±1.6) and twelve age/gender-matched controls (age 66.3±1.6) underwent 7 Tesla-MRI under Institutional Review Board approval; written informed consent was obtained from all participants in accordance with the Declaration of Helsinki. iRBD was diagnosed after neurological examination based on the International Classification of Sleep Disorders-Third Edition (ICSD-3) diagnostic criteria. Controls had no history of sleep disorders or other neurological diseases. See Supplementary Table 1 for demographic data.

MRI Acquisition

T_1-weighted MEMPRAGE image was acquired with a repetition-time (TR)=2.53s, echo times (TE)=2.39, 5.62 ms, inversion time=1.1 s, flip angle=7°, FOV=240×240×240 mm, bandwidth=332 Hz/pixel, GRAPPA factor=2, isotropic spatial resolution=0.75 mm, acquisition time=6′34′′.

Author Manuscript Author Manuscript Author Manuscript Author Manuscript

For structural connectivity analyses, diffusion-weighted spin-echo EPI (HARDI) was acquired using a custom-built 32-channel receive coil, with parameters: 82 slices, unipolar diffusion-weighting gradients, TE=66.8 msec, TR=7.4 sec, phase-encoding direction: anterior/posterior, bandwidth=1456 Hz/pixel, partial Fourier=6/8, 60 diffusion directions (b-value=2500 s/mm^2), seven interspersed "b0" images (b-value=0 s/mm^2), isotropic spatial resolution=1.7 mm, acquisition time=8′53′′. To perform distortion correction, we also acquired seven "b0" images with opposite phase-encoding direction (posterior/anterior).

Data Analysis

Definition of seed and target regions for HARDI-based connectivity analysis: As *seed regions*, we used the structural probabilistic atlas labels of 11 brainstem nuclei[5–7] relevant for iRBD/premanifest-synucleinopathy or involved in motor or arousal functions (Fig. 1B), mapped from IIT-MNI-space to native-space (using the coregistration transformations explained in Supplementary Materials). We expanded the *in-vivo* brainstem nuclei atlas, creating nine additional probabilistic nuclei labels relevant for iRBD/premanifest-synucleinopathy (Fig. 1C–D), using the same dataset as in[5], and used them as seed regions. See Supplementary Materials and Supplementary Figs. 1–9 for a detailed description of the segmentation and validation procedure.

As *target regions*, we used the probabilistic atlas labels of these 20 brainstem nuclei, the superior olivary complex[8], the inferior olivary nucleus, red nucleus, subthalamic nucleus[5] (for both brainstem nuclei seeds and targets, we thresholded the probabilistic labels at 35%), as well as the cortical/subcortical bilateral regions obtained in each subject from the MEMPRAGE Freesurfer-parcellation (mapped to native space, see Supplementary Materials). We also used as targets the hypothalamus[9] and the spinal cord (divided into ventral and dorsal parts) in IIT-MNI space; we registered these labels applying the same registration as for brainstem nuclei (see Supplementary Materials).

Single-subject HARDI-based connectivity analysis: We performed probabilistic tractography using MRtrix3 (pre-processing and tractography parameters described in Supplementary Materials). We computed a "structural-connectivity-index" (range: [0 1]) for each pair of seed-target masks (= fraction of streamlines propagated from the seed reaching the target mask).

Group HARDI-based connectivity analysis: We averaged across subjects the structural-connectivity-index of brainstem nuclei with target-regions to yield a group structural connectome of these nuclei. We displayed this connectome using a 2D circular diagram. For display purposes, Freesurfer cortical parcellations were grouped into anatomical lobes (frontal/temporal/parietal/occipital).

Statistical analysis: We ran a two-sample Shapiro-Wilk test for normality of the connectivity indices across subjects. Since at least 30.2% of the connectivity-indices did not follow a normal distribution across subjects, we used an unpaired Wilcoxon rank-sum test (two-sided, $p<0.01$) to compare the differences in connectivity indices between groups, and displayed them using 2D circular connectomes.

Author Manuscript Author Manuscript Author Manuscript Author Manuscript

Results

Figure 1C–D demonstrates the probabilistic atlas labels of nine newly delineated brainstem nuclei, and their validation.

The structural connectome of 20 brainstem nuclei (12 bilateral and eight midline nuclei, amounting to total of 32 nuclei) relevant for iRBD/premanifest-synucleinopathy demonstrated connectivity changes (specifically, in 14 out of 32 brainstem seeds) across groups ($Z = 2.6$, $p < 0.01$) mainly focused within the brainstem regions (Fig. 2A–B, see also Supplementary Figs. 10–12). Note that, except for one link with the frontal cortex, we did not achieve significant *changes* in connectivity in iRBD patients versus controls with areas other than the brainstem (Fig. 2A).

Figure 2 B–C shows connectivity maps and diagrams summarizing our results. Notably, decreased structural connectivity occurred mainly in the ponto-medullary brainstem nuclei, while increased connectivity was found in meso-pontine brainstem nuclei. The direct pathway between SubC and the spinal cord was preserved, while the indirect pathway through the medullary reticular formation displayed decreased connectivity. Interestingly, except for PnO-PnC, REM-off areas did not show differences in connectivity between groups.

Discussion

Current understanding of iRBD physiopathology knowledge derives mainly from animal studies because several factors have hampered the study of this sleep disorder in living humans, mainly lack of an atlas to precisely localize small brainstem structures in living subjects and limited sensitivity/resolution of diffusion MRI. Our work contributed to overcame both limitations, by mapping an original brainstem nuclei atlas[5–8] to high-spatial resolution HARDI at 7 Tesla in living humans. Interestingly, we found that changes in anatomical connectivity in iRBD patients were mainly restricted to specific brainstem nuclei, results that expand knowledge from animal non-isolated RBD models[3].

First, we found impaired connectivity in iRBD patients between REM-on and REM-sleep muscle-atonia areas in the medulla. This is in agreement with animal non-isolated RBD studies[10,11] showing weaker excitatory connectivity influences between REM-on regions and ventro-medullary nuclei, the latter projecting to spinal motoneurons critical for generating muscle atonia during REM-sleep (indirect pathway). In contrast, other studies[12,13] have postulated that efferences from REM-on neurons may be responsible of REM atonia mainly by direct spinal projections to interneurons that inhibit spinal motoneurons.

Second, the majority of REM-off areas did not show differences in connectivity between groups. Interestingly, studies have shown that injury to REM-off regions increases the amount of REM-sleep and fragmentation of REM-sleep[3,14–16]. Our results are aligned with observations of similar latency and percentage of REM-sleep in iRBD patients compared with controls[17].

Author Manuscript Author Manuscript Author Manuscript Author Manuscript

Third, ponto-medullary brainstem nuclei, known to be involved in REM atonia[11], showed *decreased* structural inter-connectivity, possibly related to an underlying neurodegeneration process[3,4]. In contrast, meso-pontine regions showed overall *increased* inter-connectivity and with the frontal cortex. We speculate this might be associated to compensatory mechanisms. Interestingly, diffusion MRI has proven useful to identify white matter plasticity changes in humans[18] both over short and long time scales.

Previous studies in iRBD patients demonstrate significant changes in diffusivity properties in the pons, LC, PTg, PAG and right SN[19,20]. Except for the PAG, these impairments are in line with our results. The result mismatch in the PAG might be related to different stages of iRBD progression across studies. Neuromelanin sensitive MRI in Parkinson's disease patients with RBD shows structural changes in the LC and SubC[21,22]. This agrees with our findings of structural connectivity changes of the SubC present even in prodromal stages of alpha-synucleinopathies. Further, susceptibility-weighted imaging studies in iRBD patients describe a loss of the dorsolateral nigral hyperintensity, compatible with neurodegeneration of dopaminergic neurons in nigrosome-1 (a subregion of the SN pars compacta)[23]. Interestingly, we found an overall structural connectivity increase in SN2 (compatible with pars compacta), possibly related to early compensatory changes in midbrain regions. Further studies are needed to concurrently evaluate brainstem microstructure and connectivity pathways.

Limitations of this work are the small cohort size and the indirect measure of connectivity provided by diffusion MRI-based tractography. The generated structural connectomes may give a better understanding of the involvement of brainstem nuclei in iRBD, however MRI-based tractography cannot fully solve crossing fibers, nor distinguish directionality, thus precluding inferences regarding causality. Despite this, tractography is one of the few suitable methods for studying *in-vivo* structural connectivity and our results were in line with previous literature. In the current study we did not control for the presence of white matter/periventricular hyperintensities that could be related to aging or cognitive decline. Upon the development of tractography methods able to control for these structural abnormalities, future studies might improve the connectome accuracy. Further, the small sample size did not allow us to apply statistical correction for multiple comparisons, which future studies with larger samples might be able to address. Further, future studies investigating different clinical phenotypes of alpha-synucleinopathy should add olfactory function evaluation. Finally, due to the small sample size and the lack of a comprehensive cognitive assessment, we included two iRBD patients with MOCA scores slightly below the cut-off, possibly indicating mild cognitive disturbances. Further studies might include broader neuropsychological testing better assessing cognition. Future work will develop automatic rater-independent segmentations for broader applications and to reduce segmentation time of manual delineations, which currently require several hours per subject.

In summary, these results suggest that the structural brainstem nuclei connectome is a promising tool to study and possibly assess prodromal synucleinopathy stages.

Author Manuscript Author Manuscript Author Manuscript Author Manuscript

Supplementary Material

Refer to Web version on PubMed Central for supplementary material.

Acknowledgements

Sources of funding: National-Institutes-of-Health (NIH) National-Institute-of-Biomedical-Imaging-and-Bioengineering K01-EB019474, P41-EB015896; NIH National-Institute-on-Deafness-and-other-Communication-Disorders R21-DC015888; NIH National-Institute-on-Aging R01-AG063982; NIH National-Institute-on-Neurological-Disorders-and-Stroke R21-NS108022; Massachusetts-General-Hospital Claflin-Distinguished-Scholar-Award, and Harvard-University Mind/Brain/Behavior Faculty Award. This work was also made possible by Shared-Instrumentation-Grants 1S10RR023401, 1S10RR019307, 1S10RR023043; We thank Dr. Thorsten Feiweier for providing the diffusion sequence used in this study.

Funding sources for study:

National Institutes of Health (NIH) National-Institute-of-Biomedical-Imaging-and-Bioengineering K01-EB019474 and P41-EB015896; NIH National-Institute-on-Deafness-and-other-Communication-Disorders R21-DC015888; NIH National-Institute-on-Aging R01-AG063982; NIH National-Institute-on-Neurological-Disorders-and-Stroke R21-NS108022; the Massachusetts-General-Hospital Claflin-Distinguished-Scholar-Award, and Harvard-University Mind/Brain/Behavior Faculty Award. This work was also in part made possible by the resources provided by Shared-Instrumentation-Grants 1S10RR023401, 1S10RR019307, and 1S10RR023043.

References

1. Schenck CH, Bundlie SR, Ettinger MG, Mahowald MW. Chronic behavioral disorders of human REM sleep: a new category of parasomnia. Sleep. 1986;9:293–308. [PubMed: 3505730]
2. Postuma RB, Iranzo A, Hu M, Högl B, Boeve BF, Manni R, et al. Risk and predictors of dementia and parkinsonism in idiopathic REM sleep behaviour disorder: a multicentre study. Brain. 2019;142:744–59. [PubMed: 30789229]
3. Boeve BF, Silber MH, Saper CB, Ferman TJ, Dickson DW, Parisi JE, et al. Pathophysiology of REM sleep behaviour disorder and relevance to neurodegenerative disease. Brain. 2007;130:2770–88. [PubMed: 17412731]
4. Braak H, Ghebremedhin E, Rüb U, Bratzke H, Del Tredici K. Stages in the development of Parkinson's disease-related pathology. Cell Tissue Res. 2004;318:121–34. [PubMed: 15338272]
5. Bianciardi M, Toschi N, Edlow BL, Eichner C, Setsompop K, Polimeni JR, et al. Toward an *In Vivo* Neuroimaging Template of Human Brainstem Nuclei of the Ascending Arousal, Autonomic, and Motor Systems. Brain Connectivity. 2015;5:597–607. [PubMed: 26066023]
6. Bianciardi M, Strong C, Toschi N, Edlow BL, Fischl B, Brown EN, et al. A probabilistic template of human mesopontine tegmental nuclei from in vivo 7T MRI. Neuroimage. 2018;170:222–30. [PubMed: 28476663]
7. Singh K, Indovina I, Augustinack JC, Nestor K, García-Gomar MG, Staab JP, et al. Probabilistic Template of the Lateral Parabrachial Nucleus, Medial Parabrachial Nucleus, Vestibular Nuclei Complex, and Medullary Viscero-Sensory-Motor Nuclei Complex in Living Humans From 7 Tesla MRI. Front Neurosci. 2020;13:1425. [PubMed: 32038134]
8. García-Gomar MG, Strong C, Toschi N, Singh K, Rosen BR, Wald LL, et al. In vivo Probabilistic Structural Atlas of the Inferior and Superior Colliculi, Medial and Lateral Geniculate Nuclei and Superior Olivary Complex in Humans Based on 7 Tesla MRI. Front Neurosci. 2019;13:764. [PubMed: 31440122]
9. Pauli WM, Nili AN, Tyszka JM. A high-resolution probabilistic in vivo atlas of human subcortical brain nuclei. Sci Data. 2018;5:180063. [PubMed: 29664465]
10. Luppi P-H, Clément O, Valencia Garcia S, Brischoux F, Fort P. New aspects in the pathophysiology of rapid eye movement sleep behavior disorder: the potential role of glutamate, gamma-aminobutyric acid, and glycine. Sleep Medicine. 2013;14:714–8. [PubMed: 23790501]

Author Manuscript Author Manuscript Author Manuscript Author Manuscript

11. Valencia Garcia S, Brischoux F, Clément O, Libourel P-A, Arthaud S, Lazarus M, et al. Ventromedial medulla inhibitory neuron inactivation induces REM sleep without atonia and REM sleep behavior disorder. Nat Commun. 2018;9:504. [PubMed: 29402935]
12. Lu J, Sherman D, Devor M, Saper CB. A putative flip–flop switch for control of REM sleep. Nature. 2006;441:589–94. [PubMed: 16688184]
13. Fuller PM, Saper CB, Lu J. The pontine REM switch: past and present: The pontine REM switch. The Journal of Physiology. 2007;584:735–41. [PubMed: 17884926]
14. Kaur S, Thankachan S, Begum S, Liu M, Blanco-Centurion C, Shiromani PJ. Hypocretin-2 Saporin Lesions of the Ventrolateral Periaquaductal Gray (vlPAG) Increase REM Sleep in Hypocretin Knockout Mice. Hashimoto K, editor. PLoS ONE. 2009;4:e6346. [PubMed: 19623260]
15. Sapin E, Lapray D, Bérod A, Goutagny R, Léger L, Ravassard P, et al. Localization of the Brainstem GABAergic Neurons Controlling Paradoxical (REM) Sleep. Bartell PA, editor. PLoS ONE. 2009;4:e4272. [PubMed: 19169414]
16. Arrigoni E, Chen MC, Fuller PM. The anatomical, cellular and synaptic basis of motor atonia during rapid eye movement sleep: Neural circuitry regulating REM atonia. J Physiol. 2016;594:5391–414. [PubMed: 27060683]
17. Dauvilliers Y, Schenck CH, Postuma RB, Iranzo A, Luppi P-H, Plazzi G, et al. REM sleep behaviour disorder. Nat Rev Dis Primers. 2018;4:19. [PubMed: 30166532]
18. Sampaio-Baptista C, Johansen-Berg H. White Matter Plasticity in the Adult Brain. Neuron. 2017;96:1239–51. [PubMed: 29268094]
19. Unger MM, Belke M, Menzler K, Heverhagen JT, Keil B, Stiasny-Kolster K, et al. Diffusion tensor imaging in idiopathic REM sleep behavior disorder reveals microstructural changes in the brainstem, substantia nigra, olfactory region, and other brain regions. Sleep. 2010;33:767–73. [PubMed: 20550017]
20. Scherfler C, Frauscher B, Schocke M, Iranzo A, Gschliesser V, Seppi K, et al. White and gray matter abnormalities in idiopathic rapid eye movement sleep behavior disorder: A diffusion-tensor imaging and voxel-based morphometry study. Ann Neurol. 2011;69:400–7. [PubMed: 21387382]
21. García-Lorenzo D, Longo-Dos Santos C, Ewenczyk C, Leu-Semenescu S, Gallea C, Quattrocchi G, et al. The coeruleus/subcoeruleus complex in rapid eye movement sleep behaviour disorders in Parkinson's disease. Brain. 2013;136:2120–9. [PubMed: 23801736]
22. Pyatigorskaya N, Yahia-Cherif L, Valabregue R, Gaurav R, Gargouri F, Ewenczyk C, et al. Parkinson Disease Propagation Using MRI Biomarkers and Partial Least Squares Path Modeling. Neurology. 2021;96:e460–71. [PubMed: 33277419]
23. De Marzi R, Seppi K, Högl B, Müller C, Scherfler C, Stefani A, et al. Loss of dorsolateral nigral hyperintensity on 3.0 tesla susceptibility-weighted imaging in idiopathic rapid eye movement sleep behavior disorder: Loss of Dorsolateral Nigral Hyperintensity in iRBD. Ann Neurol. 2016;79:1026–30. [PubMed: 27016314]

Author Manuscript Author Manuscript Author Manuscript Author Manuscript

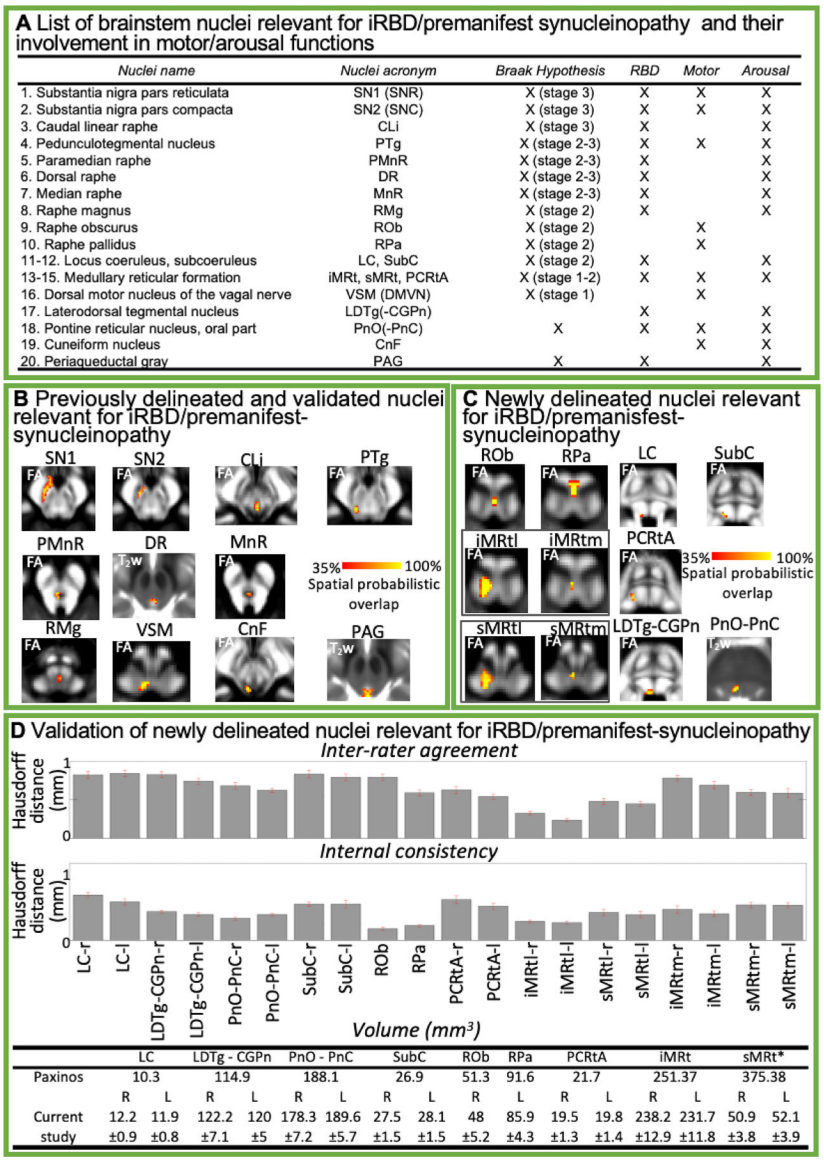

Nuclei name	Nuclei acronym	Braak Hypothesis	RBD	Motor	Arousal
1. Substantia nigra pars reticulata	SN1 (SNR)	X (stage 3)	X	X	X
2. Substantia nigra pars compacta	SN2 (SNC)	X (stage 3)	X	X	X
3. Caudal linear raphe	CLi	X (stage 3)	X		X
4. Pedunculotegmental nucleus	PTg	X (stage 2-3)	X	X	X
5. Paramedian raphe	PMnR	X (stage 2-3)	X		X
6. Dorsal raphe	DR	X (stage 2-3)	X		X
7. Median raphe	MnR	X (stage 2-3)	X		X
8. Raphe magnus	RMg	X (stage 2)	X		X
9. Raphe obscurus	ROb	X (stage 2)		X	
10. Raphe pallidus	RPa	X (stage 2)		X	
11-12. Locus coeruleus, subcoeruleus	LC, SubC	X (stage 2)	X		X
13-15. Medullary reticular formation	iMRt, sMRt, PCRtA	X (stage 1-2)	X	X	X
16. Dorsal motor nucleus of the vagal nerve	VSM (DMVN)	X (stage 1)		X	
17. Laterodorsal tegmental nucleus	LDTg(-CGPn)		X		X
18. Pontine reticular nucleus, oral part	PnO(-PnC)	X	X	X	X
19. Cuneiform nucleus	CnF			X	X
20. Periaqueductal gray	PAG	X	X		X

	LC		LDTg - CGPn		PnO - PnC		SubC		ROb	RPa	PCRtA		iMRt		sMRt*	
Paxinos	10.3		114.9		188.1		26.9		51.3	91.6	21.7		251.37		375.38	
	R	L	R	L	R	L	R	L	R	L	R	L	R	L	R	L
Current study	12.2 ±0.9	11.9 ±0.8	122.2 ±7.1	120 ±5	178.3 ±7.2	189.6 ±5.7	27.5 ±1.5	28.1 ±1.5	48 ±5.2	85.9 ±4.3	19.5 ±1.3	19.8 ±1.4	238.2 ±12.9	231.7 ±11.8	50.9 ±3.8	52.1 ±3.9

Figure 1.

A) List of brainstem nuclei relevant for iRBD and/or for synucleinopathy progression (according to the Braak hypothesis[4]). These nuclei are involved in motor and/or arousal functions (as marked in the appropriate columns). **B)** Probabilistic atlas labels of 11 brainstem nuclei relevant for iRBD/premanifest-synucleinopathy, previously published[5–7] and used as seeds and brainstem targets in this study. **C)** Additional probabilistic atlas labels of nine nuclei relevant for iRBD/premanifest-synucleinopathy generated in the current work (11 nuclei are shown because two nuclei, iMRt and sMRt, displayed two subregions, a lateral larger subregion – l – and a medial smaller subregion – m). Very good (i.e., up to 100%) spatial agreement of labels across subjects was observed indicating the feasibility of delineating the probabilistic label of these nuclei. **D)** Validation of the nuclei displayed in C). Upper row: *inter-rater agreement* of nuclei labels (bar/error bar = mean/SE modified Hausdorff distance across 12 subjects). Middle row: *internal consistency* of nuclei labels

Author Manuscript Author Manuscript Author Manuscript Author Manuscript

across subjects (bar/error bar = mean/SE modified Hausdorff distance across 12 subjects). All the nuclei displayed good spatial overlap across raters and subjects (the modified Hausdorff distance was smaller than the spatial imaging resolution, one-sided t-test, $p < 0.05$), thus validating the probabilistic nuclei template. Lower row: The *nuclei volume* from the literature (for detail information see Supplementary Table 2) and the volume (mean ± SE across subjects) of each final label in native space are shown. Note that, except for sMRt nucleus, the latter did not differ from the former (two-sided t-test, $p < 0.05$), thus further validating the generated probabilistic atlas. Nuclei abbreviations: Locus coeruleus (LC), Laterodorsal Tegmental Nucleus- Central Gray of the rhombencephalon (LDTg-CGPn), Pontine Reticular Nucleus, oral part- Pontine Reticular Nucleus, caudal part (PnO-PnC), Subcoeruleus (SubC), Raphe Obscurus (ROb), Raphe Pallidus (RPa), Parvicellular Reticular nucleus Alpha-part (PCRtA), Inferior Medullary Reticular formation (iMRt), lateral (iMRtl) and medial (iMRtm) part, Superior Medullary Reticular formation (sMRt), lateral (sMRtl) and medial (sMRtm) part.

Author Manuscript Author Manuscript Author Manuscript Author Manuscript

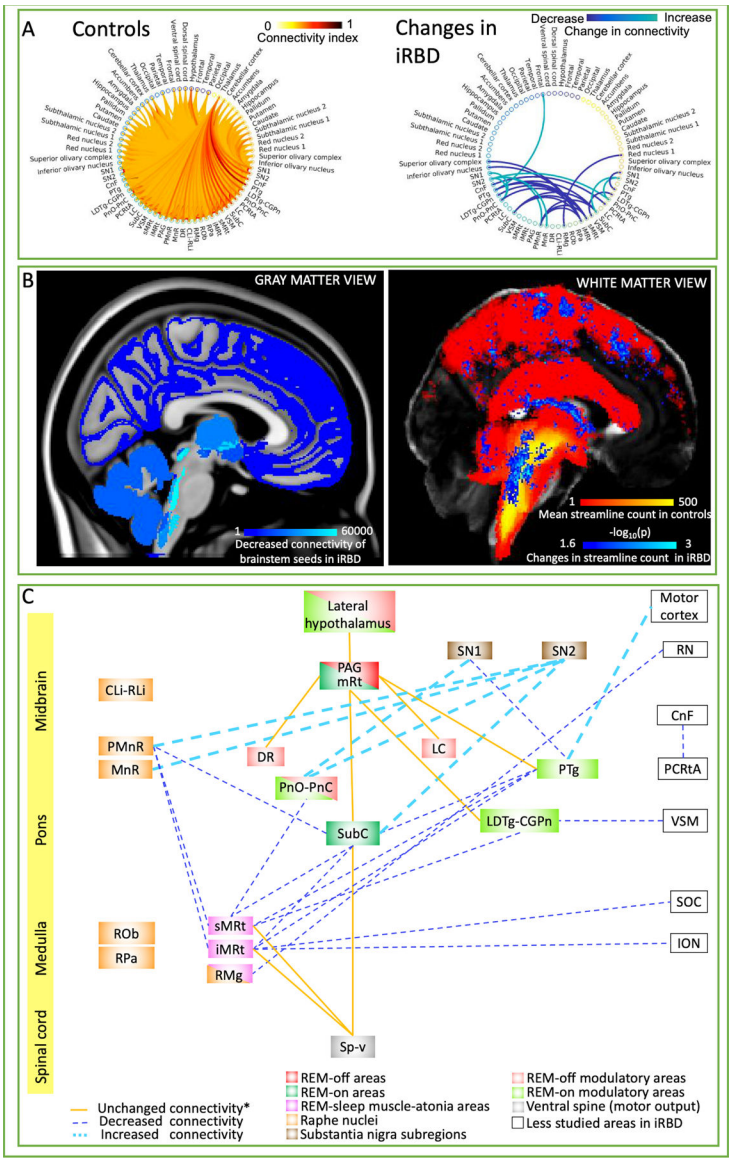

Figure 2.

A) Left: Structural tractography-based connectome of 20 brainstem nuclei relevant for iRBD/premanifest synucleinopathy (list of nuclei shown in Fig. 1A) in controls (average connectivity index across 12 controls displayed). **Right:** Statistically significant differences in structural connectivity between iRBD patients and controls (Wilcoxon test, $p < 0.01$, $n = 12$); note that, except for a significant link with the frontal cortex, alterations of connectivity pathways in iRBD occurred exclusively within brainstem nuclei. Specifically, PnO-PnC and SN showed increased reciprocal connectivity bilaterally, as well as PMnR and MnR to SN subregion 2 in the left hemisphere. In the right hemisphere iMRt, sMRt and SubC showed decreased connectivity with PMnR and contralateral PTg and SubC among other nuclei in iRBD compared to controls. Further, other nuclei such as VSM, PTg, PCRtA (on the right hemisphere) and RMg showed decreased connectivity with ipsilateral LDTg-CGPn, ipsilateral SN subregion 1, contralateral CnF and right RN subregion 1 respectively. PTg

Author Manuscript Author Manuscript Author Manuscript Author Manuscript

on the left hemisphere showed increased connectivity with ipsilateral frontal cortical areas (including central and paracentral gyrus) in iRBD compared to controls. **B) Left:** Pictorial summary of the decreased structural connectivity changes in iRBD patients in target *gray matter* regions overlaid on MNI-space. Count of decreased streamlines reaching each target region (cortical and subcortical, including brainstem nuclei), when propagated by any of our 20 brainstem nuclei seeds. **Right:** Pictorial view of *white matter* changes in iRBD versus controls. In red-yellow, the mean tract density in controls of all the brainstem nuclei relevant for iRBD/premanifest synucleinopathy. In blue-light blue, changes (both increases and decreases) in streamline count between iRBD and controls (Wilcoxon test, $p < 0.05$ uncorrected for multiple comparisons, 14 brainstem seeds) overlaid on a FA-MNI-template. **C)** Diagram summarizing the structural connectivity changes in iRBD human subjects in the present study. The iRBD relevant nuclei/regions were color-coded based on their functions as previously reported in animal and human lesion studies of non-idiopathic RBD.[3,11,17] Note that further studies are needed with regard to the homology of these anatomical areas between human and animal models. Unchanged structural connectivity between groups (indicated with *) among nuclei has been simplified to only display relevant connections for iRBD based on animal studies.[3,12] Notably, decreased structural connectivity (possibly indicating neurodegenerative mechanisms) mainly occurred in ponto-medullary brainstem nuclei previously postulated to be involved in REM atonia,[11] while increased connectivity (possibly indicating compensatory mechanisms) was found in meso-pontine brainstem nuclei. Moreover, the direct pathway between SubC and the spinal cord was preserved, while the indirect pathway through the medullary reticular formation (sMRt, iMRt) displayed decreased connectivity. Interestingly, REM-off areas (PAG, mRt (mesencephalic reticular formation), DR, LC and lateral hypothalamus) mostly did not show differences in connectivity between groups. Rather, our results showed mainly impaired connectivity in iRBD between REM-on (SubC, PnO, and REM-on modulatory areas LDTg and PTg) and REM-sleep muscle-atonia areas (mainly the medullary reticular formation nuclei sMRt, iMRt).